Hydrogen-Bonded Assembly

π-Conjugated Oligo-(*p*-phenylenevinylene) Rosettes and Their Tubular Self-Assembly**

Pascal Jonkheijm, Atsushi Miura, Magdalena Zdanowska, Freek J. M. Hoeben, Steven De Feyter, Albertus P. H. J. Schenning,* Frans C. De Schryver,* and E. W. Meijer**

Artificial cylindrical and tubular aggregates of specifically programmed molecules are of interest as sensing, transport, and bioactive systems. An important design to form these aggregates is via ring stacking and most of these stacks are composed of single-molecule rings, for example, cyclic oligopeptides.[1] Hydrogen-bond interactions between molecules are attractive candidates for obtaining well-defined supramolecular cyclic structures due to their spatial arrangement and directionality.[2] Multiple examples of these cyclic structures exist that are based on hydrogen-bonding building blocks.[3] Further aggregation of cyclic supramolecular structures into extended aggregates is, however, scarce.[4] Recently, Stupp and co-workers described an elegant example of the self-assembly of dendron rod–coil molecules into tetrameric hydrogen-bonded rosettes that further organize into nanoribbons by additional hydrogen bonding and π--π interactions.[5] Nanohelices of cadmium sulfide were made by the mineralization of these aggregates. Fenniri et al. demonstrated the formation of rosette nanotubes in which the helicity could be tuned by using amino acids.[6]

We and others have used noncovalent interactions to design π-conjugated oligomers that organize hierarchically over several length scales.[7] Self-assembled supramolecular structures of conjugated molecular building blocks are a

[*] P. Jonkheijm, F. J. M. Hoeben, Dr. A. P. H. J. Schenning, Prof. Dr. E. W. Meijer
Laboratory of Macromolecular and Organic Chemistry
Eindhoven University of Technology
P.O. Box 513, 5600 MB Eindhoven (The Netherlands)
Fax: (+31) 40-2451036
E-mail: a.p.h.j.schenning@tue.nl
e.w.meijer@tue.nl

Dr. A. Miura, M. Zdanowska, Dr. S. De Feyter, Prof. Dr. F. C. De Schryver
Department of Chemistry
Laboratory of Photochemistry and Spectroscopy
Katholieke Universiteit Leuven
Celestijnenlaan 200-F, 3001 Leuven (Belgium)
Fax: (+32) 16-327990
E-mail: Steven.DeFeyter@chem.kuleuven.ac.be
frans.deschryver@chem.kuleuven.ac.be

[**] The authors would like to thank Dr. R. Kleppinger and Dr. P. Strunz for providing SANS beam time. This work was supported by the Council for Chemical Research of the Netherlands Organization for Scientific Research (CW-NWO), the Royal Dutch Academy of Sciences (KNAW), the DWTC (through IUAP-V-03), the IWT and a fellowship of the Fund for Scientific Research—Flanders (Belgium).

Supporting information for this article is available on the WWW under http://www.angewandte.org or from the author.

  DOI: 10.1002/ange.200352790

promising class of materials to improve the solid-state organization of future optoelectronic devices.[8] Thorough research has allowed control of the photophysical properties through precise choice of the chemical structure.[9] Up to now most, if not all, π-conjugated oligomers self-assemble through the stacking of rods. To create cylindrical or, even more exciting, tubular aggregates with perfect space filling, requires another hierarchical assembly process. Here, we report on a unique and unexpected process to construct hexameric π-conjugated rosettes that self-assemble into chiral tubular objects.

In our research of quadruple-hydrogen-bonded dimeric oligomers,[7d] we analyzed two oligo-(*p*-phenylenevinylene) (OPV) precursors bearing a diamino triazine moiety (**OPVT3**, **OPVT4**; Figure 1) with scanning tunneling microscopy (STM) to obtain detailed information about self-assembly at surfaces. Unexpectedly, the STM images showed chiral hexameric rosette structures lying flat on the surface, with the diamino triazine moieties pointing to the center forming hydrogen bonds (Figure 2).[10] The trimer and tetramer are next to the diamino triazine motif, and are equipped with a tridodecyloxy "wedge" end group and substituted with two or four enantiomerically pure (*S*)-2-methylbutoxy side chains on the OPV backbone. Being the precursors for oligomers studied earlier, their syntheses were published elsewhere.[7d,11] The STM images were acquired at the solid–liquid interface using graphite as substrate and 1-phenyloctane as solvent.[12] The lengths of the bright rods correspond to the conjugated backbone of OPV, in which individual phenyl rings are sometimes resolved. Similarly, as observed before, two out of three dodecyloxy chains reside in the darker areas.[13] The rosettes are ordered in rows and form a hexagonal two-dimensional (2D) crystal lattice with alkyl chains interdigitating with adjacent rosettes. The cavity of the rosette has an estimated diameter of approximately 0.7 nm. The packing parameters (Figure 2e and f) were determined as follows: $a_1 = 55.4 \pm 0.7$ Å, $a_2 = 56.3 \pm 0.8$ Å, $\alpha = 60 \pm 5°$ for **OPVT3**, and $a_1 = 60.3 \pm 0.5$ Å, $a_2 = 61.5 \pm 0.6$ Å, $\alpha = 60 \pm 4°$ for **OPVT4**. Although **OPVT3** and **OPVT4** appear to order in a similar way—oblique unit cells, rosette structure, specific orientation of alkyl chains and OPV backbone with respect to graphite symmetry axes, a comparable angle between the OPV backbone and the dodecyloxy chain—the organization of the molecules within a single rosette surprisingly differs (Figure 2c and d). The rosettes of **OPVT3** and **OPVT4** have different "rotation directions", as shown by the orientation of the OPV backbones, although they only differ in length and, hence, the number of stereocenters. In addition, the relative orientation of rows of rosettes with respect to the main crystallographic axes of graphite shows opposite 2D chirality ($+17.7 \pm 1.7°$ and $-2.3 \pm 0.8°$ for **OPVT3** and **OPVT4**, respectively). Calculations show that the free volume of the **OPVT4** rosettes is a minimum in the case of counterclockwise (CCW) helical rosettes and therefore expected to be more stable, which is observed experimentally. However, a CCW rosette of **OPVT3** would be destabilized by the steric interactions of the OPV and dodecyloxy chains; hence the clockwise (CW) rosette structure can be explained.

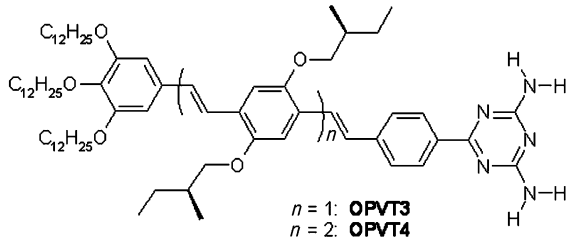

Figure 1. Molecular structures of **OPVT3** and **OPVT4**.

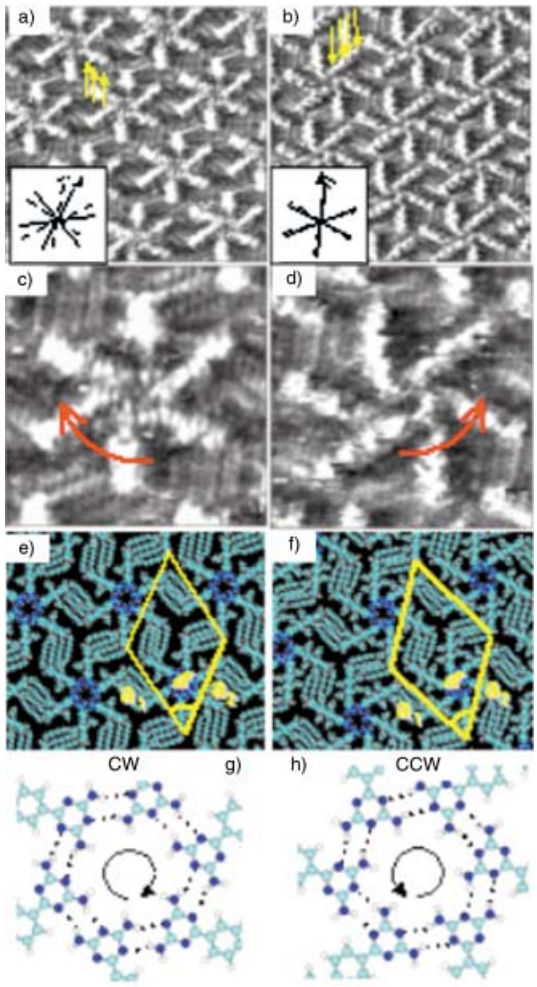

Figure 2. a, b) STM images of **OPVT3** (14.4×14.4 nm^2, $V_{set} = -0.50$ V, $I_{set} = 0.50$ nA), and **OPVT4** (18.4×18.4 nm^2, $V_{set} = -0.50$ V, $I_{set} = 0.45$ nA) monolayers at the solid–liquid interface using graphite as the substrate and 1-phenyloctane as the solvent. Yellow arrows point to intramolecularly resolved phenyl rings of the OPV backbone. Insets show the propagation direction of rosette lattices (solid line) and the main symmetry axes of graphite substrate (dashed line); c, d) close-up images of **OPVT3** and **OPVT4** rosettes. Red arrows indicate the "rotation direction" of the rosette; e, f) molecular models of an **OPVT3** and **OPVT4** monolayer; g, h) Representation of clockwise (CW) and counterclockwise (CCW) rosette structures showing the respective hydrogen-bonding patterns. Experimentally, the CCW rosette is observed for **OPVT4** and the CW rosette for **OPVT3**.

With the STM results in hand, it is intriguing to study the behavior of the molecules in solution and to search for the self-assembly of the rosettes into well-defined space-filling tubules. The UV/Vis absorption spectra of **OPVT3** and **OPVT4** in chloroform show structureless bands at $\lambda_{max} =$ 408 and 430 nm, respectively. The fluorescence maxima are positioned at $\lambda_{em\,max} = 470$ and 501 nm, respectively. The absorption and fluorescence data are characteristic for molecularly dissolved oligomers and the maxima are red-shifted when the conjugation length increases.[14] The UV/Vis absorption spectrum in heptane (5×10^{-5} M) shows a blue shift of the main band to $\lambda_{max} = 421$ nm for **OPVT4** (Figure 3a) and a red shift on the onset of the absorption. This behavior is typical for aggregated OPV derivatives.[7d] Similar spectral changes were observed in other apolar alkanes like pentane and dodecane. A similar shift in the onset of the absorption band is only observed for **OPVT3** at higher concentrations, while the absorption maximum remains unchanged.[15] The fluorescence intensity of **OPVT3** and **OPVT4** in heptane (Figure 3b) is reduced and strongly red-shifted to $\lambda_{max} = 510$ and 530 nm, respectively.

A bisignated circular dichroism (CD) effect for **OPVT4** (Figure 3c) is observed exhibiting a positive Cotton effect [+] at higher energy ($\lambda_{max,[+]} = 387$ nm) and a negative Cotton effect [−] at lower energy ($\lambda_{max,[-]} = 428$ nm). The zero-crossing lies at $\lambda = 400$ nm, which is not related to a maximum in absorption for **OPVT4** in heptane. Surprisingly, the bisignated CD spectrum of **OPVT3** (Figure 4a) is opposite to **OPVT4** ($\lambda_{max,[-]} = 380$ and $\lambda_{max,[M+]} = 428$ nm). The zero-crossing of the Cotton effect of **OPVT3** is positioned at $\lambda =$ 405 nm, which is close to the absorption maximum of the chromophore indicating strong exciton coupling. It is tempting to compare the opposite CD effects for the two molecules with the opposite chirality of the two molecules at the graphite surface. However, for **OPVT4** we found an inversion of the Cotton effect with time (Figure 4c). At 288 K, an almost complete conversion was obtained within 80 min ($\lambda_{max,[-]} = 410$ and $\lambda_{max,[+]} = 448$ nm) accompanied by a shifted zero-crossing to 422 nm, which is in close proximity of the absorption maximum. Annealing of **OPVT3** did not lead to sign reversal, only an increase of the Cotton effect was observed, while the zero-crossing is even closer to the absorption maximum. The sign reversal of **OPVT4** shows first-order kinetics with a rate constant of $k = 5.6 \times 10^{-4}\ s^{-1}$ (Figure 4c, inset). The helix that is initially present is presumably the kinetically controlled aggregate, while the helix that is finally formed is the thermodynamically stable form.[16] Hence, the exciton-coupled CD spectra for **OPVT3** and **OPVT4** are the same in the thermodynamically stable structures.

The aggregation process was further studied by temperature-dependent measurements (Figure 3). For **OPVT4** in heptane, the fluorescence maximum shifts from $\lambda_{max} = 530$ to 495 nm upon heating while the absorption maximum shift from $\lambda_{max} = 420$ to 430 nm. The values at high temperature are close to those found in chloroform, which indicates molecularly dissolved species. The melting transition temperature from the aggregated state to molecular dissolved species lies

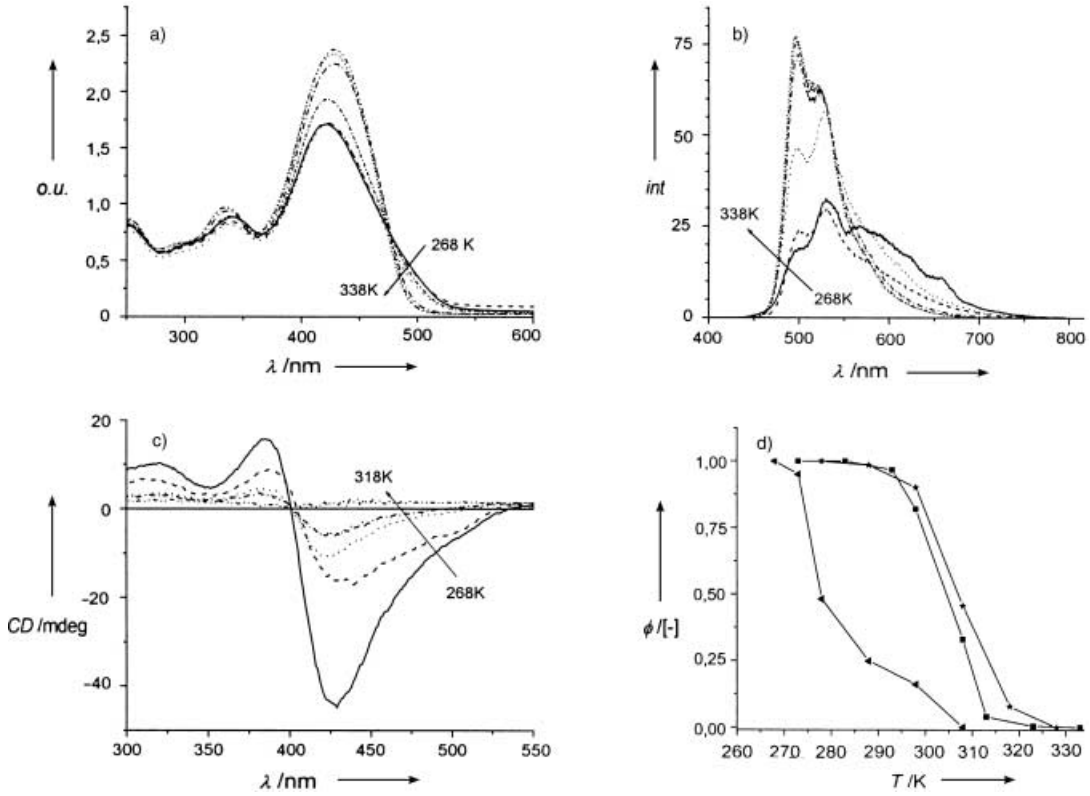

Figure 3. Temperature-variable a) UV/Vis, b) fluorescence, and c) CD spectra of **OPVT4** in heptane solution (5×10^{-5} M); d) melting-transition curves with fraction of aggregated species versus temperature based on CD (◂), fluorescence (⋆), and UV/Vis (■) data for **OPVT4**.

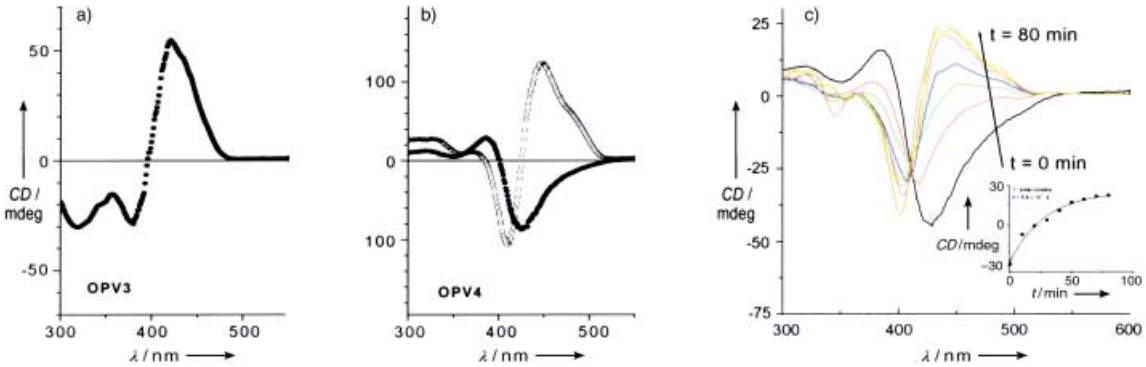

Figure 4. CD spectra of a) **OPVT3** (2.5×10^{-4} M) and b) **OPVT4** (5×10^{-5} M) in annealed heptane solutions recorded after maintaining at 293 K for 10 min (●) and for 24 hr (○); c) time-dependent CD spectra of **OPVT4** in steps of 10 min at 288 K. The inset shows the change of the CD intensity at $\lambda = 450$ nm versus time fitted to first-order kinetics.

at $T_m = 305$ K (Figure 4d). Remarkably the Cotton effect disappears earlier ($T_m = 280$ K, Figure 4d) than the disassembly. This behavior indicates a two-step aggregation process; first a transition from molecular dissolved species into achiral stacked structures that further develop into helical stacks. This aggregation process is distinct from our earlier findings on related OPVs.[7d] Hence, it is proposed that several secondary interactions act independently in the self-assembly process, as often seen in the assembly processes in aqueous media.[17]

Small-angle neutron scattering (SANS) and atomic force microscopy (AFM) measurements of **OPVT4** assemblies were used to study the shape of the supramolecular aggregates in solution, and as transferred from solution to a graphite surface. SANS data of **OPVT4** (5×10^{-4} M in dodecane, $T = 288$ K) showed a linear slope of -1 with a side maximum in the plot of the scattering vector versus the scattering intensity (Figure 5d) that is representative of cylindrical aggregates. The scattering data at low angles do not show a change in slope, which indicates that the persistence length of the aggregates reaches at least 185 nm at minimum experimental Q. From the position of the side maximum at high angles, the radius of the cross section can be estimated as 7 nm. AFM experiments were performed on drop-cast films from heptane solutions (5×10^{-5} M) of **OPVT4** on graphite.[18] Isolated cylindrical aggregates were revealed with lengths up to 10 μm (Figure 5a and b). Presumably during the transfer process the stacks present in solution further self-assemble in the stack direction yielding longer aggregates in the solid state. Crossovers of separate fibers are often observed. The width of the stacks is uniformly ~40 nm. Corrected for broadening of the lateral dimensions due to tip-convolution effects, the actual width is about 10 nm.[19] The heights of the stacks was determined to be ~6.4 nm from the height profile (Figure 5c), which is more reliable since soft tapping conditions were applied. This thickness is in agreement with the SANS data and corresponds well to the diameter of the hydrogen-bonded hexamers found by STM pointing to fibers consisting of stacked rosettes. The measured length and diameter show that the aspect ratio of the aggregates can be as high as 1500. We did not observe helicity

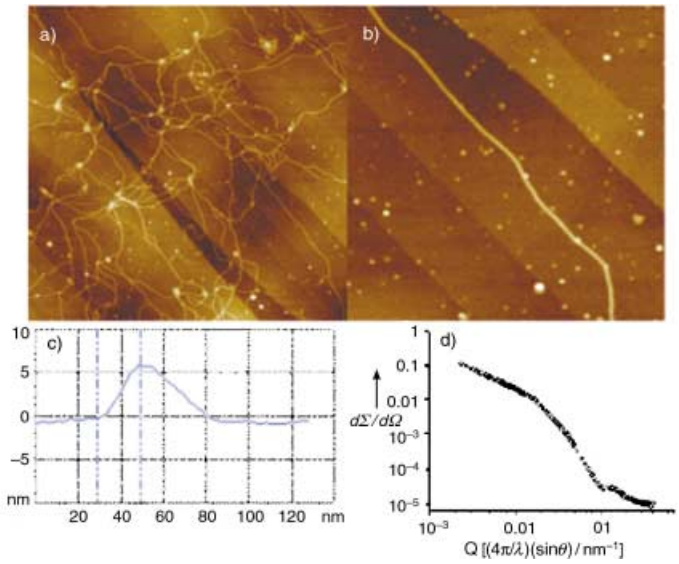

Figure 5. AFM images of drop-cast **OPVT4** solutions in heptane (5×10^{-5} M) on graphite: a) 6.3×6.3 μm^2 (z range: 30 nm) and b) 804×804 nm^2 (z range: 20 nm); c) height profile of a fibril; d) SANS data revealing columnar structures in dodecane solutions of **OPVT4**.

in the stacks. Helicity might still be present due to a pitch length that is too small to be detected or that the dodecyloxy tails that shield the stacks are not helically ordered.

Despite the temptation to relate the rotational direction or supramolecular chirality of the chiral rosettes as detected by CD and STM, it is in our view impossible at the present time. CD spectroscopy probes primarily rosette–rosette interactions whereas in STM the packing of rosettes is predominantly determined by rosette–graphite interactions. The formation of the tubules, however, can be proposed based on the earlier work of other supramolecular aggregates.[20] The OPVs with diamino triazine moieties self-assemble hierarchically; first forming hexameric rosettes by hydrogen-bond formation, which subsequently develops into stacks aided by π–π interactions of the phenylenevinylene groups. Once organized into stacks that are highly space-filled as compared to self-assembled rods, the chiral side chains induce

supramolecular helicity. It is proposed that the cyclic hexameric rosettes are not fully planar at the triazine terminus, which results in a propeller arrangement that allows interplanar hydrogen-bond interactions form rosette to rosette, thus locking the rosettes within the tubules.[4d,17] Upon heating, these hydrogen bonds are broken, which results in a loss of the Cotton effect. Time-dependent CD measurements show that the locking of rosettes is a very delicate process.

This work demonstrates guidelines for programming π-conjugated molecules into self-assembled tubular aggregates in solution and in the solid state.[21] Weak interactions that determine the packing of molecules in a crystal can be applied to the supramolecular organization in solution. The tubules of 6.4 nm in diameter and with perfect space filling are still soluble due to the apolar shell that surrounds the stacks. Since the cavity of the rosettes contains amines and has a diameter of nearly 1 nm this seems an ideal channel for transportation. Current research focuses on studying the behavior of the interior of the tubular stacks and their possible connection with the well-defined and ordered π-conjugated periphery.

Received: September 4, 2003 [Z52790]

Keywords: helices · hydrogen bonds · noncovalent interactions · self-assembly · supramolecular chemistry

[1] For a recent review and references therein: D. T. Bong, T. D. Clark, J. R. Granja, M. R. Ghadiri, *Angew. Chem.* **2001**, *113*, 1016; *Angew. Chem. Int. Ed.* **2001**, *40*, 988.

[2] G. A. Jeffrey, *An Introduction to hydrogen bonding*, Oxford University, Oxford, **1997**.

[3] For example: a) J. A. Zerowski, G. M. Whitesides, *J. Am. Chem. Soc.* **1994**, *116*, 4298; b) A. Ranganathan, V. R. Pedireddi, C. N. R. Rao, *J. Am. Chem. Soc.* **1999**, *121*, 1752; c) L. J. Prins, F. De Jong, P. Timmerman, D. N. Reinhoudt, *Nature* **2000**, *408*, 181; d) G. M. Whitesides, E. E. Simanek, J. P. Mathias, C. T. Seto, D. N. Chin, M. Mammen, D. M. Gordon, *Acc. Chem. Res.* **1995**, *28*, 37; e) M. L. Highfill, A. Chandrasekaran, D. E. Lynch, D. A. Hamilton, *Cryst. Growth Des.* **2002**, *1*, 15; f) S. V. Kolotuchin, S. C. Zimmerman, *J. Am. Chem. Soc.* **1998**, *120*, 9092; g) A. Marsh, M. Silvestri, J.-M. Lehn, *Chem. Commun.* **1996**, 1527.

[4] For example: a) N. Kimizuka, S. Fujikawa, S. Kuwahara, T. Kunitake, A. Marsh, J.-M. Lehn, *Chem. Commun.* **1995**, 2103; b) H. Schönherr, V. Paraschiv, S. Zapotoczny, M. Crego-Calama, P. Timmerman, C. W. Frank, G. J. Vancso, D. N. Reinhoudt, *Proc. Natl. Acad. Sci. USA* **2002**, *99*, 5025; c) G. Gottarelli, E. Mezzina, G. P. Spada, F. Carsughi, G. di Nicola, P. Mariani, A. Sabaticci, S. Bonazzi, *Helv. Chim. Acta* **1996**, *79*, 220; d) W. Yang, X. Chai, L. Chi, X. Liu, Y. Cao, R. Lu, Y. Jiang, X. Tang, H. Fuchs, T. Li, *Chem. Eur. J.* **1999**, *5*, 1144.

[5] a) E. D. Sone, E. R. Zubarev, S. I. Stupp, *Angew. Chem.* **2002**, *114*, 1781; *Angew. Chem. Int. Ed.* **2002**, *41*, 1706; b) E. R. Zubarev, M. U. Pralle, E. D. Sone, S. I. Stupp, *J. Am. Chem. Soc.* **2001**, *123*, 4105.

[6] H. Fenniri, B.-L. Deng, A. E. Ribbe, *J. Am. Chem. Soc.* **2002**, *124*, 11064.

[7] a) F. S. Schoonbeek, J. H. van Esch, B. Wegewijs, D. B. A. Rep, M. P. de Haas, T. M. Klapwijk, R. M. Kellog, B. L. Feringa, *Angew. Chem.* **1999**, *111*, 1486; *Angew. Chem. Int. Ed.* **1999**, *38*, 1393; b) F. Würthner, C. Thalacker, A. Sautter, *Adv. Mater.* **2000**, *12*, 562. c) A. P. H. J. Schenning, A. F. M. Kilbinger, F. Biscarini, M. Cavallini, H. J. Cooper, P. J. Derrick, W. J. Feast, R. Lazzaroni, Ph. Leclère, L. A. McDonell, E. W. Meijer, S. C. J. Meskers, *J. Am. Chem. Soc.* **2002**, *124*, 1269; d) A. P. H. J. Schenning, P. Jonkheijm, E. Peeters, E. W. Meijer, *J. Am. Chem. Soc.* **2001**, *123*, 409; e) R. B. Prince, L. Brunsveld, E. W. Meijer, J. S. Moore, *Angew. Chem. Int. Ed.* **2000**, *112*, 234; *Angew. Chem. Int. Ed.* **2000**, *39*, 228; f) A. Ajayaghosh, S. J. George, V. K. Praveen, *Angew. Chem.* **2003**, *115*, 346; *Angew. Chem. Int. Ed.* **2003**, *42*, 332; g) A. P. H. J. Schenning, J. van Herrikhuyzen, P. Jonkheijm, Z. Chen, F. Würthner, E. W. Meijer, *J. Am. Chem. Soc.* **2002**, *124*, 10252; h) H. Engelkamp, S. Middelbeek, R. J. M. Nolte, *Science* **1999**, *284*, 785; i) V. Percec, M. Glodde, T. K. Bera, Y. Mlura, I. Shlyanovskaya, K. D. Singer, V. S. K. Balagurusamy, P. A. Helney, I. Schnell, A. Rapp, H.-W. Spiess, S. D. Hudson, H. Duan, *Nature* **2002**, *417*, 384.

[8] U. Mitschke, P. Bäuerle, *J. Mater. Chem.* **2000**, *10*, 365; b) H. Sirringhaus, P. J. Brown, R. H. Friend, M. M. Neilsen, K. Bechgaard, B. M. W. Langeveld-Voss, A. J. H. Spiering, R. A. J. Janssen, E. W. Meijer, P. Herwig, D. M. de Leeuw, *Nature* **1999**, *401*, 685; c) L. Schmidt-Mende, A. Fechtenkötter, K. Müllen, E. Moons, R. H. Friend, J. D. MacKenzie, *Science* **2001**, *293*, 1119.

[9] R. E. Martin, F. Diederich, *Angew. Chem.* **1999**, *111*, 1440; *Angew. Chem. Int. Ed.* **1999**, *38*, 1350.

[10] Interestingly, the formation of hydrogen-bonded hexameric structures of melamines was previously proposed in literature: C. Thalacker, F. Würthner, *Adv. Funct. Mater.* **2002**, *12*, 209.

[11] The synthesis of **OPVT3** will be published elsewhere: P. Jonkheijm, F. J. M. Hoeben, R. Kleppinger, J. van Herrikhuyzen, A. P. H. J. Schenning, E. W. Meijer, *J. Am. Chem. Soc.*, in press.

[12] For a recent review and references therein: S. De Feyter, F. C. De Schryver, *Chem. Soc. Rev.* **2003**, *32*, 139.

[13] A. Gesquière, P. Jonkheijm, A. P. H. J. Schenning, E. Mena-Osteritz, P. Bäuerle, S. De Feyter, F. C. De Schryver, E. W. Meijer, *J. Mater. Chem.* **2003**, *13*, 2164.

[14] E. Peeters, A. Marcos, S. C. J. Meskers, R. A. J. Janssen, *J. Chem. Phys.* **2000**, *112*, 9445.

[15] Concentration-dependent UV/Vis measurements in dodecane also show that **OPVT4** starts to aggregate at 5×10^{-6} M whereas **OPVT3** starts at 2.5×10^{-5} M.

[16] M. M. Bouman, E. W. Meijer, *Adv. Mater.* **1995**, *7*, 385.

[17] L. Brunsveld, H. Zhang, M. Glasbeek, J. A. J. M. Vekemans, E. W. Meijer, *J. Am. Chem. Soc.* **2000**, *122*, 6175.

[18] With STM and AFM we observe different types of structures on graphite. This might be the result of the different solvents applied. Another possibility could be that in case of the AFM studies, a monolayer of rosettes is initially formed, and that on top of this layer fibers are present. We have not investigated this in detail.

[19] The broadening can be estimated by using a simple model based on a spherical tip apex (radius R) and a rectangular cross section of the fiber (height H) with 2(H(2R-H))/0.5 as in P. Samori, V. Francke, T. Mangel, K. Müllen, J. Rabe, *Opt. Mater.* **1998**, *9*, 390. For the present height and a terminal radius of commercial tips of 20 nm the broadening is about 29 nm. Therefore, the "true" width is obtained by subtracting the broadening from the apparent width and is about 10 nm.

[20] L. Brunsveld, B. J. B. Folmer, E. W. Meijer, R. P. Sijbesma, *Chem. Rev.* **2001**, *101*, 4071.

[21] J.-M. Lehn, *Chem. Eur. J.* **2000**, *6*, 2097.

